

Genome-wide investigation of the OR gene family in *Helicoverpa armigera* and functional analysis of OR48 and OR75 in metamorphosis development

Yanli Li^a, Qichao Chai^a, Ying Chen^b, Yujia Ma^c, Yongcui Wang^a, Junsheng Zhao^{a,*}

^a Institute of Industrial Crops, Shandong Academy of Agricultural Sciences, Jinan 250100, Shandong, China

^b Crop Research Institute, Shandong Academy of Agricultural Sciences, Jinan 250100, Shandong, China

^c College of Life Sciences, Shandong Normal University, Jinan 250300, Shandong, China

ARTICLE INFO

Keywords:

Odorant receptors
20-Hydroxyecdysone (20E)
Insulin
Phylogeny
Functional analysis
Helicoverpa armigera

ABSTRACT

The cotton bollworm, *Helicoverpa armigera*, is a significant global agricultural pest, particularly detrimental during its larval feeding period. Insects' odorant receptors (ORs) are crucial for their crop-feeding activities, yet a comprehensive analysis of *H. armigera* ORs has been lacking, and the influence of hormones on ORs remain understudied. Herein, we conducted a genome-wide study and identified 81 ORs, categorized into 15 distinct groups. Analyses of protein motifs and gene structures revealed both conservation within groups and divergence among them. Comparative gene duplication analysis between *H. armigera* and *Bombyx mori* highlighted different duplication patterns. We further investigated subcellular localization and protein interactions within the odorant receptor family, providing valuable insights for future functional and interaction studies of ORs. Specifically, we identified that *OR48* and *OR75* were abundantly expressed during molting/metamorphosis and feeding stages, respectively. We demonstrated that 20E induced the upregulation of *OR48* via EcR, while insulin upregulated *OR75* expression through InR. Moreover, 20E induced the translocation of *OR48* to the cell membrane, mediating its effects. Functional studies involving the knockdown of *OR48* and *OR75* revealed their roles in metamorphosis development, with *OR48* knockdown resulting in delayed pupation and *OR75* knockdown leading to premature pupation. *OR48* can promote autophagy and apoptosis in fat body, while *OR75* can significantly inhibit apoptosis and autophagy. These findings significantly contribute to our understanding of OR function in *H. armigera* and shed light on potential avenues for pest control strategies.

1. Introduction

Lepidoptera, the second largest order in the insect class, encompasses a diverse array of species, from silk worms to moths, along with numerous agricultural pests [1]. Among these pests, the cotton bollworm, *H. armigera*, stands out for its significant threat to cotton and various crops worldwide. Understanding the molecular mechanisms and physiological processes governing the development of *H. armigera* remains paramount. Throughout its lifecycle, *H. armigera* undergoes six larval instars, pupal stage, and adulthood, with pivotal roles played by 20-hydroxyecdysone (20E) and insulin [2]. During the metamorphosis of *H. armigera*, the larval tissues, particularly the fat body, are degraded through autophagy [3] and apoptosis [4,5]. The larval stage, encompassing feeding and metamorphic phases, poses the most substantial risk to crops. *H. armigera* larvae are notorious for their voracious appetite, feeding on a spectrum of crops including cotton, corn, soybeans, and

peanuts [6]. Therefore, unraveling the differential gene expression between feeding and non-feeding stages holds significant promise for effective pest management strategies.

Odorant receptors (ORs) are integral to the olfactory system, responsible for detecting odorants and initiating the sense of smell. These receptors, classified within the superfamily of G protein-coupled receptors (GPCRs), feature seven hydrophobic membrane-spanning regions and play a pivotal role in olfactory recognition [7]. Beyond odor recognition, recent research has shed light on the involvement of olfactory receptors in glucose metabolism. They contribute to maintaining blood glucose homeostasis by regulating hormone secretion, fat metabolism, and insulin sensitivity [8].

In *H. armigera*, a multitude of ORs and odorant binding proteins (OBPs) have been identified, each contributing to various physiological processes. While transcriptome sequencing revealed sixty-five candidate ORs in *Helicoverpa armigera* [9], a comprehensive analysis of all ORs

* Corresponding author.

E-mail address: zhaojunsheng@saas.ac.cn (J. Zhao).

<https://doi.org/10.1016/j.ijbiomac.2024.134646>

Received 30 April 2024; Received in revised form 24 July 2024; Accepted 8 August 2024

Available online 10 August 2024

0141-8130/© 2024 Elsevier B.V. All rights are reserved, including those for text and data mining, AI training, and similar technologies.

within the genome is yet to be undertaken. Hence, our study aims to screen highly expressed odorant receptors during feeding and non-feeding periods through genomic and transcriptome analyses, offering insights into their roles and potential implications for pest control.

HarmORs serve not only as key players in the olfactory perception of adult insects [10], but also exert significant influence over larval food selection and avoidance mechanisms. For instance, Gr180, a bitter taste receptor abundantly expressed in the upper beak of *H. armigera* larvae, responds to plant secondary substances such as coumarin, which act as feeding inhibitors for many plants [11]. Moreover, certain HarmORs participate in the migration behavior of *H. armigera*. Take OBP3/OBP6, for instance, which facilitate flight activity by interacting with lipid molecules [12]. This discovery reveals the potential role of HarmORs in insect energy metabolism and motility. However, the exploration of other functions of HarmORs remains somewhat limited, and the *in vivo* perception of endogenous hormones is not thoroughly understood. Both human sex hormones and insect ecdysone fall under the category of steroid hormones. Although studies have highlighted the crucial roles of sex hormones in empathy-related measures and odor perception [59,60], a definitive mechanism remains elusive.

To investigate the effect of hormones on ORs, we utilized *H. armigera* as our experimental model, analyzing ORs within its genome and conducting phylogenetic analysis. Through transcriptome screening, *OR75* and *OR48* were identified to be upregulated by insulin and 20E during feeding and metamorphic stages, respectively. Knocking down *OR75* accelerated the larval-pupal transition, and significantly promoted apoptosis and autophagy in fat body. Whereas knocking down *OR48* delayed pupation, inhibited apoptosis and autophagy in fat body. Further investigation revealed that 20E increased *OR48* expression via the nuclear receptor EcR, while insulin upregulated *OR75* expression through its receptor InR.

2. Material and methods

2.1. Genome-wide analysis of OR genes in *H. armigera*

The HMMER program (<http://www.hmmerr.org/>) was employed to search the *H. armigera* genome using the 7tm Odorant receptor domain (PF02949) with an e-value threshold of less than 1e-5. Subsequently, all putative proteins were subjected to confirmation using SMART (<http://smart.emblheidelberg.de/>), Pfam (<http://pfam.xfam.org/>), and the NCBI CDD database (<http://www.ncbi.nlm.nih.gov/cdd>). Predictions of the theoretical isoelectric point (pI) and molecular weight (MW) for each OR protein were conducted using the online tool ExPASy (<https://www.expasy.org/>) [36]. Furthermore, Wolf PSORT (<https://wolfsort.hgc.jp/>) was utilized to estimate the subcellular localization of ORs [37].

2.2. Phylogenetic, chromosomal mapping, gene duplication, conserved motif, gene structure, and protein interaction analyses

The HarmOR family proteins underwent multiple sequence alignment using MEGA11 (<http://www.megasoftware.net/>). Subsequently, a phylogenetic tree was established using the Neighbor-joining (NJ) approach with a bootstrap of 1000 replications [38]. The resulting NJ tree was visualized using iTOL v6 (<http://itol.embl.de/>) [39]. The chromosomal location map of the OR genes was generated using MapChart software [40], and further refined using Adobe Illustrator CS6 software for clarity. BLAST analysis was employed to examine the duplication pattern of each OR gene. Conserved motifs were estimated using MEME Suite (<http://meme-suite.org/>). Collinearity relationships between chromosomes in the genome were assessed using McscanX software [41], and the syntenic relationship of duplicated genes was depicted using the Circos program [42]. The HarmOR protein interaction network was established using STRING (<https://string-db.org/>) [43] and visualized using Cytoscape.

2.3. Split-ubiquitin membrane yeast two-hybrid (MYTH) assay

MYTH assay was performed essentially as described previously. Briefly, the yeast strain NMY 51 was co-transformed with the bait (pBT3-N derivatives) and prey (pPR3-N/C derivatives) plasmids. Transformants were plated onto a synthetic dropout medium lacking tryptophan and leucine (SD-LW) and a selective medium lacking tryptophan, leucine, histidine, and adenine (SD-LWHA). For MYTH assay constructs, primers were listed in Supplementary Table S1.

2.4. Insects and cells

Specimens of *H. armigera* were sourced from Keyun Biology (China) and maintained on a custom artificial diet, with regular food changes. Larvae were reared at a temperature of 26 ± 1 °C under 14:10-h light/dark cycle. To ensure data consistency and reliability, samples with identical morphological features were randomly selected. HaEpi cells, previously derived from the epidermis of fifth instar larvae [44], were cultured at 27 °C in Grace's insect cell culture medium (11300-043, Gibco, USA) supplemented with 10 % fetal bovine serum (FBS; 16,140,063, Gibco, USA).

2.5. Real-time quantitative reverse transcription PCR (RT-qPCR)

Total RNA was extracted from larvae, pupae, and adults using TRIzol reagent (Tiangen Biotech, Beijing, China), followed by cDNA synthesis using a reverse transcription kit (R323-01, Vazyme Biotech, Nanjing, China). RT-qPCR was performed using ChamQ Universal SYBR qPCR Master Mix (Q711-02, Vazyme Biotech, Nanjing, China) on a LightCycle 480 instrument (Roche), with primer pairs listed in Table S1. β -Actin served as the internal standard, and relative expression levels were computed using the $2^{-\Delta\Delta Ct}$ approach. Data indicate the mean of 3 biological replicates and were analyzed using the formula $R = 2^{-\left(\text{sample } \Delta Ct - \text{control } \Delta Ct\right)}$ [13].

2.6. Hormonal induction

The 20E (16,145, Cayman Chemical, MI, USA) was diluted to 10 mg/mL in DMSO (D8371, Solarbio, Shanghai, China), while insulin (P3376-400 IU, Beyotime Biotechnology, Shanghai, China) was diluted to 100 ng/ μ L in sterile PBS (pH 7.4, 1.8 mM KH_2PO_4 , 10 mM Na_2HPO_4 , 2.7 mM KCl, and 140 mM NaCl). Sixth-instar larvae, aged 6 h, were injected with varying concentrations and time gradients of 20E and insulin, with DMSO and PBS serving as respective controls. Total mRNA was then extracted and quantitatively analyzed using RT-qPCR. HaEpi cells were exposed to 5 μ g/mL insulin and 5 μ M 20E [14,15], while PBS and DMSO were employed as solvent controls. The molar concentration of 20E was determined using the formula $c = \rho/M$, where c represents the molar concentration of 20E, ρ is the mass of 20E in 100 μ L of hemolymph, and M is the molar mass of 20E (480.63 g/mol) [16].

2.7. RNA interference (RNAi) in larvae

The T7 promoter was ligated to the 5'-end of the interfering primer, initiating amplification of the targeted gene segment. The T7-RiboMAX-Express-RNAi-System (Promega, USA) was used for dsRNA synthesis. The concentrations of dsRNA were assessed using a NanoDrop-2000 spectrophotometer, and its quality was evaluated by 1 % agarose gel electrophoresis. Similar larvae were chilled on ice for 30 min until they became immobile. Then, 3 μ g dsRNA was injected into each larva at the 4th appendage once every 24 h for 3 injections. Each injection was performed in triplicate with 30 larvae each time. An equal amount of *dsGfp* was utilized as a control. The effect of RNAi was assessed through RT-qPCR.

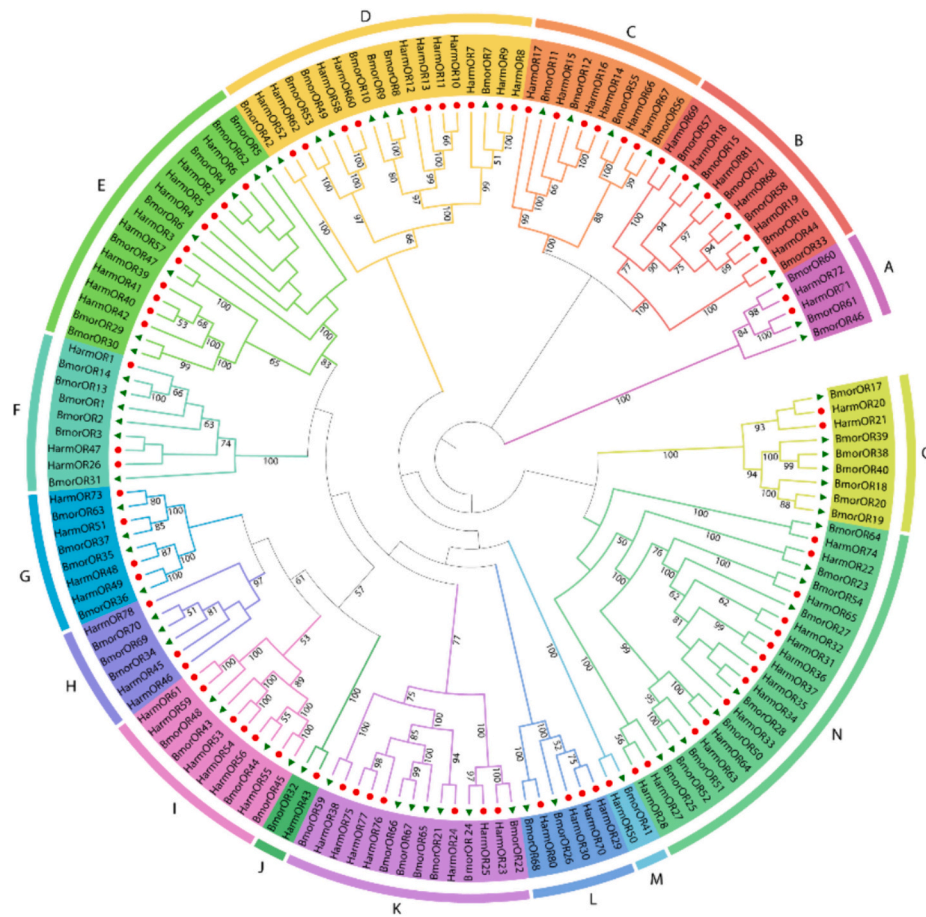


Fig. 1. Phylogenetic tree of 81 OR sequences of *H. armigera* and 71 ORs of *B. mori*. Multiple sequence alignment of ORs of *H. armigera* and *B. mori* was performed using ClustalW. MEGA11 was used to construct the Neighbor-Joining (NJ) tree with 1000 bootstrap replicates. Various colors indicate different groups of OR genes.

2.8. Histological analysis

The larval midgut and fat body was isolated, followed by fixation with 4 % paraformaldehyde at 4 °C overnight and gradual dehydration. Subsequently, the tissue was embedded in molten paraffin and sliced into 7- μ m sections using a paraffin-slicing machine (Leica RM2245). These sections were then affixed to gelatin-coated glass slides, followed by drying at 42 °C overnight. After dewaxing, the tissue sections underwent gradual rehydration, followed by digestion with 20 mM proteinase K for 10 min at 37 °C. H&E staining was performed on the tissue sections using the H&E staining kit (C0105S, Beyotime Biotechnology, Shanghai, China). The paraffin-embedded fat body was cut into 4 μ m fragments, fixed on glass slides, and then dried at 60 °C for 2 h, stained according to the YF488 TUNEL apoptosis detection instructions (T6013, US EVERBRIGHT INC, Suzhou, China). Servicebio company conducted the transmission electron microscopy (TEM) scanning. A fluorescence microscope (Olympus BX51) was employed to visualize positive signals.

2.9. Overexpression of OR proteins in HaEpi cells

The open reading frames (ORFs) of *HarmOR48* and *HarmOR75* were amplified using their corresponding primers (Table S1) and subsequently inserted into the pIEx-4-GFP-His plasmid. Recombinant vectors were constructed wherein the C-terminal of the target protein was fused with GFP and histidine tags. The plasmid (5 μ g/mL) was transfected into HaEpi cells using the QuickShuttle-enhanced transfection reagent (KX0110042, Biodragon Immunotechnologies, Beijing, China) until the cells reached 70–80 % confluence.

2.10. Chromatin immunoprecipitation (ChIP)

The *EcR-RFP-His* plasmid was introduced into HaEpi cells cultured in 6-well plates at 70 % confluency and incubated for 72 h. Subsequently, the cells were treated with 5 μ M 20E for 6 h, and DMSO was utilized as a control. The ChIP Assay Kit (P2078, Beyotime Biotechnology, Shanghai, China) was employed for subsequent assays. The chromatin was cross-linked by adding 1 % formaldehyde (252,549, Sigma-Aldrich, Saint Louis, USA) to the cells and incubating them for 10 min at 37 °C, followed by quenching with 125 mM glycine (P2078–2, Beyotime Biotechnology, Shanghai, China) for 5 min. The cells were then rinsed twice with ice-cold PBS containing 1 mM PMSF (A100754, Sangon Biotech, Shanghai, China) and collected via centrifugation. After sonication to shear the chromatin into fragments of 200 to 1000 bp, the supernatant was collected and diluted with ChIP dilution buffer (P2078–3, Beyotime Biotechnology, Shanghai, China) containing 1 mM PMSF. The diluted chromatin was incubated with Protein A + G Agarose-salmon sperm DNA (P2078–1, Beyotime Biotechnology, Shanghai, China) at 4 °C for 1 h. Following centrifugation, a portion of the supernatant was retained as an input sample for RT-qPCR, while the remaining supernatant from the experimental group was exposed to antibodies against RFP (AE020, ABclonal Technology, Wuhan, China) or mouse control IgG (AC011, ABclonal Technology, Wuhan, China) at 4 °C overnight, and then with Protein A + G Agarose-salmon sperm DNA at 4 °C for 2 h. The immunocomplex was washed sequentially with low-salt-buffer (P2078–4, Beyotime Biotechnology, Shanghai, China), high-salt-wash-buffer (P2078–5, Beyotime Biotechnology, Shanghai, China), LiCl-wash-buffer (P2078–6, Beyotime Biotechnology, Shanghai, China), and twice with TE-buffer (P2078–7, Beyotime Biotechnology,

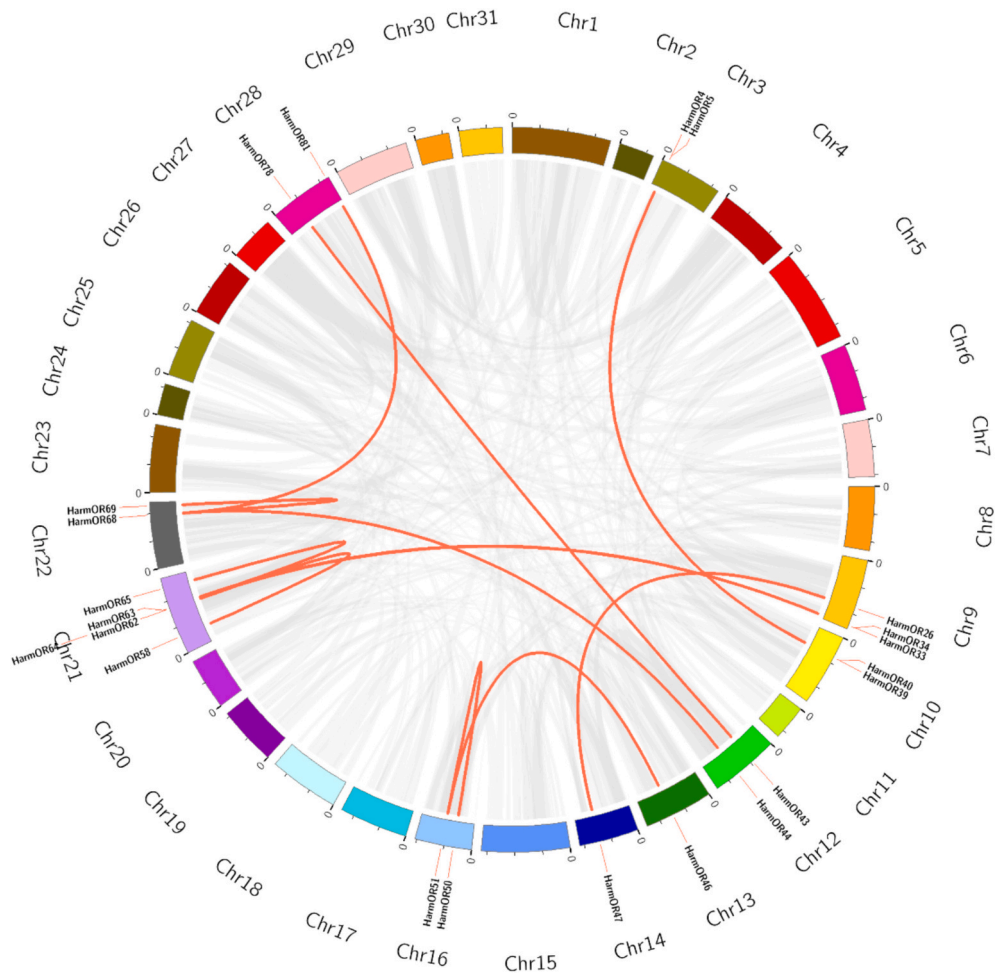


Fig. 2. Distribution of OR gene pairs of chromosomes in intra-genomics of *H. armigera*. The boxes represent chromosomes, and the red lines represent OR homologous pairs.

Shanghai, China), and the DNA was eluted in elution buffer (100 mM NaHCO₃, 1 % SDS). The DNA-protein cross-links were reversed for 4 h at 65 °C and exposed to RNase A (ST576, Beyotime Biotechnology, Shanghai, China) for 1 h at 37 °C and proteinase K (A510453, Sangon Biotech, Shanghai, China) for 2 h at 45 °C, with the input sample processed similarly. DNA purification was carried out, followed by analysis using RT-qPCR to determine EcR-USP1-binding elements in the OR48 promoter region using the OR48 PF/OR48 PR primer pairs (Table S1). IgG was employed as a positive control.

2.11. Statistical analysis

The statistical analysis involved ANOVA for multiple comparisons or Student's *t*-test for paired comparisons. Error bar in each figure represents the mean \pm SD of 3 independent experiments. Statistical difference was assessed using a two-tailed paired test. Asterisks denote statistical significance (* $p < 0.05$, ** $p < 0.01$, and *** $p < 0.001$). GraphPad v7.0 was utilized for figure generation. Different lowercase letters denote significant differences ($p < 0.05$) in the ANOVA test.

3. Results

3.1. Identification of OR genes in *H. armigera*

In total, 81 OR genes were identified in *H. armigera* through a Hidden-Markov-Model (HMM) search within the genome. Further verification was carried out utilizing the SMART, Pfam, and NCBI CDD.

The sequences were named according to their chromosomal location. These OR genes encoded protein sequences spanning from 281 (HarmOR48) to 840 (HarmOR79) amino acids in length, with the majority falling around the 400 amino acid mark. The molecular weights (MWs) of these proteins ranged from 32.17 (HarmOR48) to 97.39 (HarmOR79) kilodaltons (kDa), while their theoretical isoelectric points (pIs) varied between 5.11 (HarmOR4) and 9.77 (HarmOR81). Subcellular localization predictions were made using the WoLF PSORT website, revealing that most ORs were situated within the plasma membrane. For detailed information, such as gene ID, chromosome location, gene locus, sequence length, subcellular location, pI, and MW, refer to Supplementary Table S2.

3.2. Phylogenetic analysis of OR genes

To explore the evolutionary relationships among different OR genes, we established a neighbor-joining phylogenetic tree using both *HarmOR* and *Bombyx mori* OR genes. The phylogenetic analysis encompassed a total of 81 *HarmOR* genes and 71 *BmorOR* genes, as depicted in Fig. 1 and Table S3. By examining sequence similarities and evolutionary patterns, the OR genes were categorized into 15 primary groups labeled A to O (Fig. 1). Notably, Group N comprised the largest contingent of *HarmOR* genes, totaling 14, whereas Groups J and M exhibited the smallest representation, each containing only one *HarmOR* gene.

3.3. Chromosome locations and duplications of HarmORs

The chromosomal distribution of HarmORs within the genome was elucidated by extracting chromosomal data and employing MapChart for mapping [40]. Thus, 81 HarmOR genes were non-randomly and unevenly distributed across 22 chromosomes, with no HarmOR gene identified on chromosomes 2, 4, 11, 17, 20, 23, 29, 30, or 31 (Fig. S1). Chromosome 9 harbored the highest count of HarmOR genes, totaling 16, followed by chromosomes 5 and 21, which contained 10 and 8 genes, respectively. The remaining chromosomes, namely 7, 8, 12, 13, 15, 16, 18, 22, 25, 26, 27, and 28, each accommodated 2 to 4 HarmOR genes. Only one HarmOR gene was mapped onto chromosomes 1, 6, 14, 19, and 24.

Given the pivotal role of duplication events in gene family expansion during evolution, a gene duplication analysis was conducted within the *H. armigera* genome. Four gene pairs (*HarmOR50/HarmOR51*, *HarmOR58/HarmOR62*, *HarmOR63/HarmOR65*, *HarmOR68/HarmOR69*) were identified as tandem duplicated and nine gene pairs (*HarmOR4/HarmOR39*, *HarmOR5/HarmOR40*, *HarmOR26/HarmOR47*, *HarmOR33/HarmOR63*, *HarmOR34/HarmOR64*, *HarmOR43/HarmOR78*, *HarmOR44/HarmOR68*, *HarmOR46/HarmOR51*, *HarmOR68/HarmOR81*) were identified as segmentally duplicated (Fig. 2). These findings indicate that tandem repeat events and segmental duplication events can regulate the expansion of HarmORs.

Additionally, we investigated the collinear relationship between *H. armigera* and *B. mori*. A total of 48 collinear pairs of homologous genes were identified between HarmORs and *BmorORs* (Fig. S2 and Table S6). The selection pressure exerted on OR gene duplication was evaluated through the Ka/Ks ratio (Table S7). Typically, a Ka/Ks value < 1 signifies purifying selection, a Ka/Ks ratio = 1 suggests neutral evolution, and a Ka/Ks value > 1 indicates directional selection [45,46]. Notably, all the Ka/Ks values were < 1, indicating that these HarmOR genes underwent purifying selection throughout the extensive evolutionary process.

3.4. Gene structure analysis and conserved motifs

The gene architecture serves as both the structural framework and evolutionary signature of the gene, offering insights into the gene family's structural evolution. As illustrated in Fig. S3, all HarmOR genes exhibit a combination of exons and introns. The majority of HarmOR members (95 %) display 4–12 exons, with exceptions such as *HarmOR14*, *HarmOR21*, and *HarmOR79*, which respectively feature 20, 18, and 14 exons. Conversely, *HarmOR38* presents a minimalistic structure with only 2 exons and 1 intron. Within the same cluster, members often share similar sequence features, indicating their close evolutionary proximity (Table S4).

To elucidate the diversity within the OR family genes, we conducted predictive analysis of conserved motifs. We identified 10 conserved motifs (Motif 1 to Motif 10) within the HarmOR family, varying in length from 15 to 96 amino acids (Fig. S4). The protein sequences corresponding to these motifs can be found in Table S5. The majority of HarmOR proteins (96.3 %) harbor 2–6 conserved motifs, though exceptions such as *HarmOR8*, *HarmOR21*, and *HarmOR79* exhibit an expanded motif repertoire, containing 10 and 12 motifs respectively. Notably, certain motifs, such as Motif 1 and Motif 2, demonstrate widespread presence across most HarmORs, albeit with a few exceptions such as *HarmOR23* and *OR75–77*. Moreover, closely related HarmOR proteins within neighboring clades of phylogenetic trees tend to exhibit identical or similar motif compositions, suggesting a correlation between evolutionary relatedness and motif structure.

3.5. Interaction network of HarmOR proteins

A protein interaction network was established to explore the interactions between HarmOR and other proteins in *H. armigera* (Fig. S5).

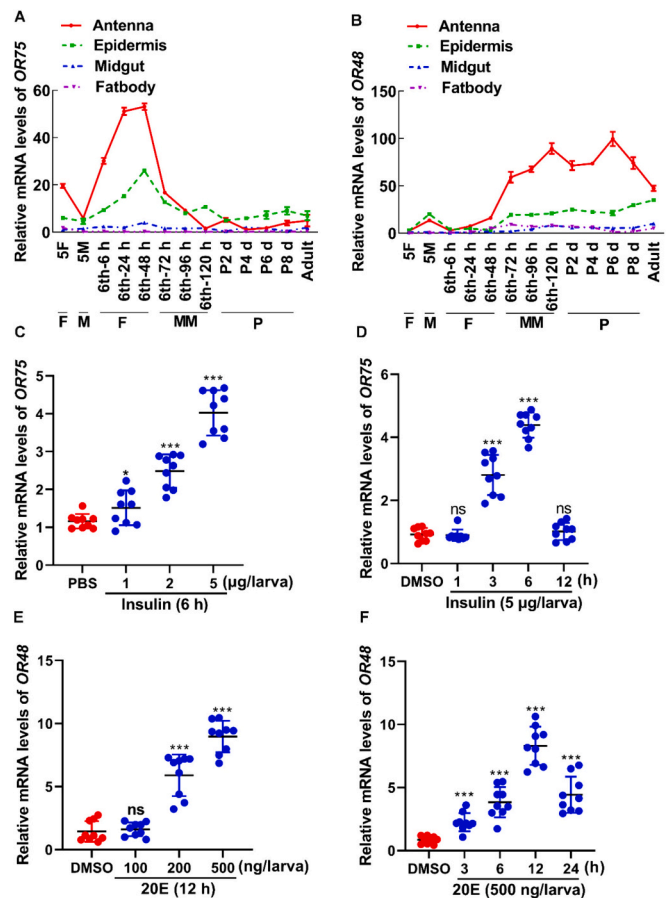


Fig. 3. Insulin upregulated the expression of OR75 and 20E upregulated the expression of OR48. (A–B) Relative expression levels of OR75 and OR48 in the antenna, epidermis, midgut and fat body detected by RT-qPCR. 5F, fifth instar feeding larvae; 5 M, fifth instar molting larvae; 6th-6 h–120 h, sixth instar larvae at different stages; P2 d to P8 d, 0- to 8-day-old pupae; Adult, adult. F, feeding; M, molting; MM, metamorphic molting; P, pupae. (C–D) Relative expression levels of OR75 in antenna after insulin injection over dosage and time. (E–F) Relative expression levels of OR48 in antenna after 20E injection over dosage and time. Paired data were statistically analyzed using Student's *t*-test; ns indicates no significance; asterisks indicate significant differences (**p* < 0.05, ***p* < 0.01, ****p* < 0.001). The bars in the figures represent the mean standard deviation (SD) for three separate biological experiments.

Thirteen proteins were mapped onto this network, comprising nine from the HarmOR family and four from other protein families. These findings imply that the functions of certain HarmOR proteins may rely on interactions with other proteins. Furthermore, the interactions between HarmOR50 and predicted interactive proteins (IR25a, GluD1, GPRgr22, and GPRgr24) were confirmed by MYTH assay (Fig. S6). The relevant information of interacting proteins, including predicted binding scores, was presented in Table S8.

3.6. Identification of OR75 and OR48 as targets of insulin and 20E upregulation

To identify ORs exhibiting high expression levels during feeding and metamorphosis stages, we compared the transcriptome data of the epidermis at these respective stages in *H. armigera*. 70 ORs were detected in the epidermis. OR75 emerged as highly expressed during the feeding stage (6th-24 h), whereas OR48 exhibited upregulated expression during the metamorphosis stage (6th-96 h) (Fig. S7A). Eight ORs were chosen for qRT-PCR to corroborate the transcriptome findings (Fig. S7B). The expression profiles of OR75 and OR48 were further examined elucidate

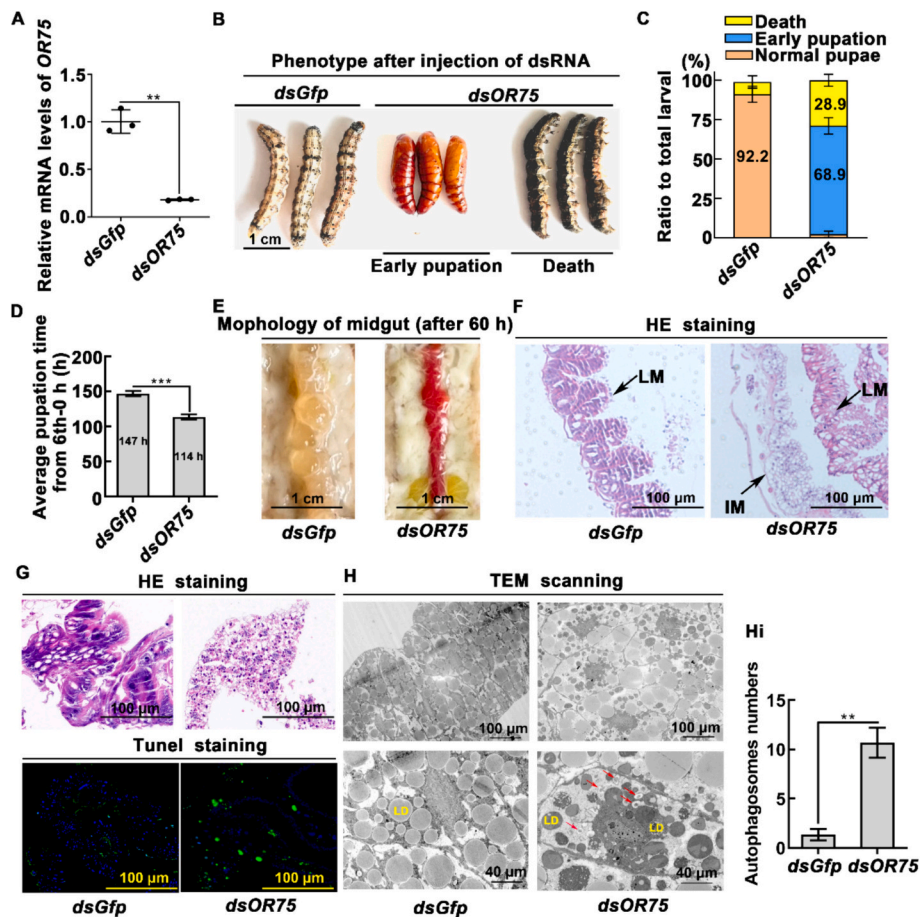


Fig. 4. *OR75* knockdown via RNAi in larvae accelerated pupation time. (A) Efficacy of *OR75* knockdown in larvae by RT-qPCR analysis (sixth instar 6 h larva for the first *dsGfp* or *dsOR75* injection, 24 h later for the second injection, 3 μ g dsRNA/larva). (B) Phenotypes after injection of *dsGfp* and *dsOR75*; the ruler represents 1 cm. (C) The phenotypes ratio after *OR75* knockdown. (D) Average pupation time after knockdown of *Gfp* and *OR75*. (E) Morphology of the midgut. (F) H&E staining was used to evaluate the morphological changes of the midgut after *Gfp* and *OR75* knockdown. (G) H&E staining and TUNEL staining showing fat body morphology after *Gfp* and *OR75* knockdown. The green fluorescence in TUNEL staining shows the apoptotic cell area in the fat body, while the blue represents the nucleus of the cell. (H) TEM observation after injection with *dsOR75* in the fat body. The red arrows indicated autophagosomes. LD: lipid droplets. (Hi) The number of autophagosomes contained in three different images. The area of each image is approximately 0.09 mm². Paired data were statistically analyzed using Student's *t*-test; asterisks indicate significant differences (***p* < 0.01, ****p* < 0.001). The bars in the figures represent the mean standard deviation (SD) for three separate biological experiments.

their roles in insect development. *OR75* demonstrated elevated expression levels during feeding stages (6th-6 h to 6th-48 h), while *OR48* displayed heightened expression during wandering and pupal stages (6th-72 h to P8) (Fig. 3A and B). These results suggest distinct roles for different odorant receptors during feeding and non-feeding periods, with *OR75* primarily active during feeding and *OR48* predominantly involved during non-feeding stages.

To elucidate the mechanisms underlying the function of different ORs at various stages, we determined the impact of insulin and 20E by treating the hemocoel of 6th-6 h larvae with varying concentrations of these substances. The findings demonstrated that insulin, in a concentration/time-dependent fashion, upregulated the mRNA level of *OR75* (Fig. 3C and D), while 20E, in a concentration/time-dependent fashion, upregulated the mRNA level of *OR48* (Fig. 3E and F).

3.7. Knockdown of *OR75* advances the larval-pupal transition

To assess the involvement of *OR75* in the insulin signaling pathway *in vivo*, we utilized RNAi to knock down *OR75* expression in larvae by injecting *dsOR75* into the hemocoel of 6th-6 h larvae. Subsequent RT-qPCR analysis confirmed successful *OR75* knockdown in the antenna (Fig. 4A). Notably, knockdown of *OR75* led to accelerated pupation, occurring approximately 33 h earlier compared to the control group

(Fig. 4B-D). Additionally, larvae in the *dsOR75* group exhibited a red appearance in the midgut, indicative of larval midgut programmed cell death during metamorphosis, a phenomenon not observed in the *dsGfp* group (Fig. 4E). This indicates that larvae in the *dsOR75* group initiated metamorphosis earlier than the control group. HE staining further revealed the formation of imaginal midgut after *dsOR75* injection, whereas no such formation occurred after *dsGfp* injection for 60 h (Fig. 4F). After knocking down *OR75* promoted the dissociation of fat body and enhanced apoptosis signals (Fig. 4G). TEM showed that compared with *dsGfp*, knocking down *OR75* increased the number of autophagosomes (including degenerated organelles or degraded lipid droplets) in fat body (Fig. 4H-Hi), indicating that *OR75* can significantly inhibit apoptosis and autophagy.

3.8. Knockdown of *OR48* delays pupation

To verify the functional role of *OR48* in 20E-mediated pupation, we injected dsRNA targeting *OR48* into the hemocoel of sixth instar larvae at 6 h to knock down *OR48* expression. Significant knockdown of *OR48* was found in the larval antenna compared to the *dsGfp* control (Fig. 5A). Following *OR48* knockdown, larvae exhibited delayed pupation compared to those receiving *dsGfp* (Fig. 5B). The survival rate after *OR48* knockdown was 68.9 %, with a normal pupation rate of 3.3 % and

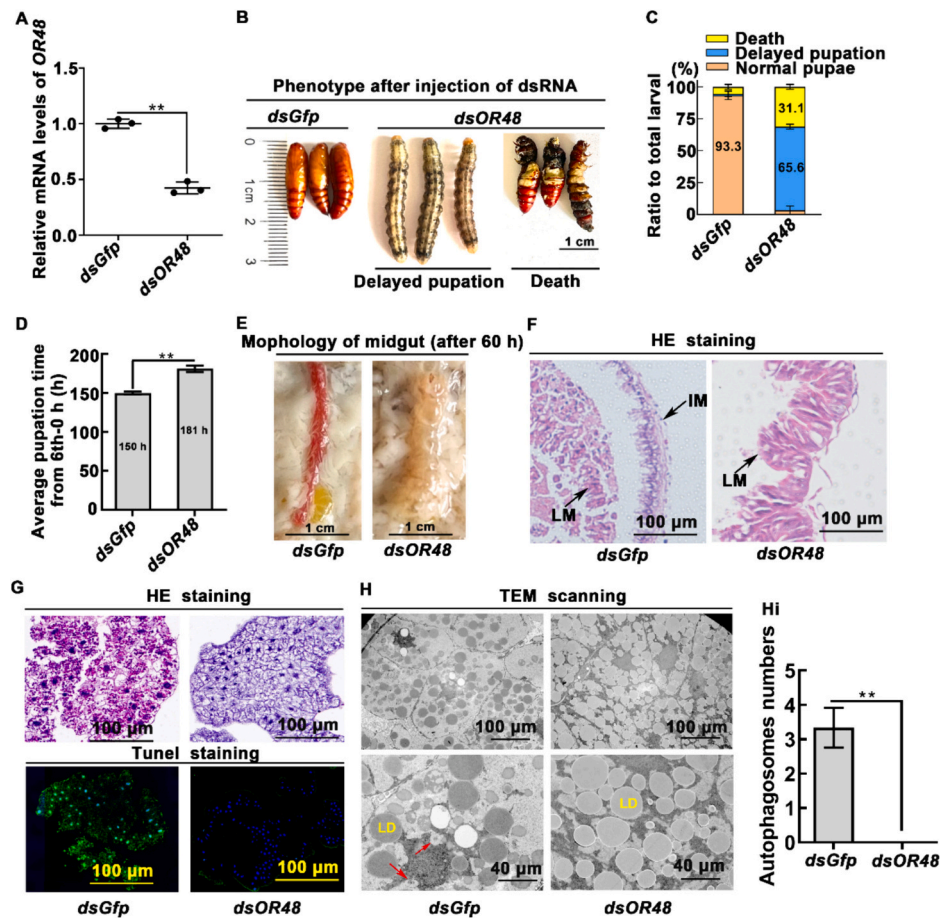


Fig. 5. OR48 knockdown via RNAi in larvae delayed pupation. (A) Efficacy of OR48 knockdown in larvae by RT-qPCR analysis (sixth instar 6 h larva for the first *dsGfp* or *dsOR48* injection, 24 h later for the second injection, 3 μ g dsRNA/larva). (B) Phenotypes after injection of *dsGfp* and *dsOR48*; the ruler represents 1 cm. (C) The phenotypes ratio after OR48 knockdown. (D) Average pupation time after knockdown of *Gfp* and OR48. (E) Morphology of the midgut. (F) H&E staining was used to evaluate the morphological changes of the midgut after *Gfp* and OR48 knockdown. (G) H&E staining and TUNEL staining showing fat body morphology after *Gfp* and OR48 knockdown. The green fluorescence in TUNEL staining shows the apoptotic cell area in the fat body, while the blue represents the nucleus of the cell. (H) TEM observation after injection with *dsOR48* in the fat body. The red arrows indicated autophagosomes. LD: lipid droplets. (Hi) The number of autophagosomes contained in three different images. The area of each image is approximately 0.09 mm². Paired data were statistically analyzed using Student's *t*-test; asterisks indicate significant differences (***p* < 0.01). The bars in the figures represent the mean standard deviation (SD) for three separate biological experiments.

a delayed pupation rate of 65.6 %, significantly differing from the *dsGfp* control ($p < 0.01$, Fig. 5C). Statistical analysis revealed a pupation delay of 31 h after *dsOR48* injection compared to *dsGfp* (Fig. 5D). As opposed to the *dsGfp* group, larvae in the *dsOR48* group did not exhibit a red appearance in the midgut (Fig. 5E), indicating a delayed entry into metamorphosis compared to the control group. HE staining indicated that while midgut remodeling occurred in the *dsGfp* group, imaginal midgut development had not yet commenced in the *dsOR48* group (Fig. 5F). After knocking down OR48, fat body dissociation was inhibited, lipid droplets no longer decomposed and decreased, and apoptosis signals weakened (Fig. 5G). TEM showed that compared with *dsGfp*, knocking down OR48 resulted in a reduction of typical autophagosomes encapsulated by a single or double membrane (Fig. 5H-Hi). This indicated that OR48 can promote autophagy and apoptosis in fat body.

3.9. 20E promotes OR48 localization on cell membrane

To investigate the impact of 20E and insulin on the subcellular localization of OR48 and OR75, we examined their distribution within the cell. Antibody detection revealed that in HaEpi cells treated with DMSO as a control, OR48 was predominantly localized in the cytosol. However, upon 20E stimulation, OR48 exhibited distribution in both the

cytoplasm and cell membrane (Fig. 6A). Similarly, OR75 was found to be localized in both the cytoplasm and cell membrane under the PBS control conditions. Notably, OR75 maintained its localization in both compartments upon insulin stimulation (Fig. 6B). These observations suggest that both OR48 and OR75 exert their functions within both the cell membrane and cytoplasm. Furthermore, OR48 appears to undergo translocation to the cell membrane specifically under 20E stimulation.

3.10. Regulation of OR48 by 20E via *EcR* and OR75 by insulin via *InR*

The putative promoter sequence for each OR gene was defined as the upstream 2 kb region. Upon analyzing the OR48 promoter, a conserved ecdysone-response-element (EcRE) binding site was identified, characterized by the sequence 5'-AAGCTCGGTGAAACC-3' (Fig. 7A). Knockdown of *EcR*, encoding the 20E nuclear receptor, resulted in decreased OR48 expression (Fig. 7B). Furthermore, the ChIP assay demonstrated that 20E enhances OR48 transcription by facilitating *EcR* binding to EcRE (Fig. 7C). These findings suggest that 20E stimulates OR48 expression through its nuclear receptor. Similarly, to investigate the upregulation of OR75 expression by insulin, *dsInR* was administered to 6th-6 h larvae to suppress insulin receptor expression, with *dsGfp* serving as a control. The expression of OR75 was reduced following *InR* knockdown (Fig. 7D), indicating that insulin promotes OR75 expression

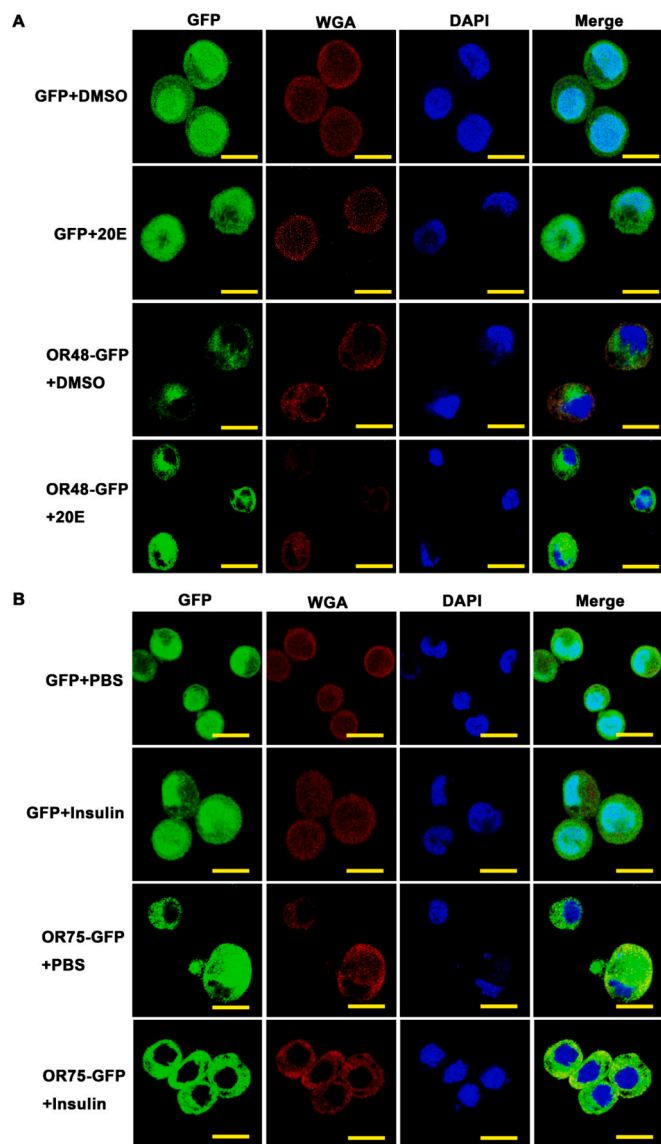


Fig. 6. 20E promotes OR48 localization on cell membrane. (A-B) Cell membrane localization of overexpression of overexpressed GFP and ORs. 20E: 5 μ M for 6 h and DMSO as control of 20E. Insulin: 5 μ g/mL, for 1 h and PBS as control of insulin. Red: the cell membrane was marked by wheat germ agglutinin (WGA). Green: green fluorescence from GFP and various ORs fused with GFP. Blue: nucleus stained with 4'-6-diamidino-2-phenylindole dihydrochloride (DAPI). Merge, overlapped green, blue, and red fluorescence. Observed by confocal microscope. Bar, 20 μ m.

through InR.

4. Discussion

Odorant receptors (ORs) play a vital role in insect feeding. Previous research has indicated that the divergence in taste receptors employed by larvae and adults forms the foundation for food preference. However, the impact of endogenous hormones remains largely unexplored. In this study, we systematically analyzed all ORs in *H. armigera* and identified OR75 and OR48 as being upregulated by insulin and 20E, respectively, during feeding and molting stages.

4.1. Characterization of OR genes in *H. armigera*

ORs, initially found by Richard Axel and Linda Buck in 1991,

represent the largest subset of GPCR superfamily. Although humans possess approximately 400 of these receptors, mice harbor over 1000 OR genes, contrasting starkly with the mere 58 OR genes identified in *Plutella xylostella* [47–50]. In this work, we identified 81 OR genes in *H. armigera* and categorized them into 15 distinct groups. This indicated that a substantial diversity within the OR gene family, which was crucial for the species' ability to detect a wide range of chemical signals. The expansion of the OR gene family in *H. armigera* has been marked by rapid proliferation, yet the underlying evolutionary mechanisms remain largely elusive. Various molecular processes drive gene duplication, with resultant duplicates either forming tandem clusters or dispersing across the genome. Furthermore, genomic rearrangements and transpositions can disrupt and scatter tandemly duplicated genes [51]. Our findings indicate that both tandem replication and segmental duplication contribute to the expansion of ORs in *H. armigera*. The chromosomal distribution of OR genes exhibits considerable variability across species. In mice, these genes are dispersed throughout the genome, existing either as solitary entities or clustered on almost all chromosomes [52,53]. In our study, we found that ORs in *H. armigera* do not cluster on specific chromosomes, with OR clusters being predominantly observed in Hymenoptera insects, a phenomenon uncommon among other insect species [22,54]. This observation aligns with previous research findings. Further exploration of regulatory motifs within OR genes enhances our comprehension of their regulatory mechanisms and their role in shaping the diversity of olfactory experiences.

4.2. The evolution of OR gene family

The OR gene family has undergone significant expansion and diversification across various species, including vertebrates and insects, each following unique evolutionary trajectories and functional adaptations [17–19]. In vertebrates, OR genes are encoded by a multigene family that has expanded and diversified extensively, contributing to the vast array of receptors expressed by olfactory sensory neurons [20].

In insects, particularly ants, the OR gene family has undergone significant expansion, enhancing their highly developed olfactory systems. This expansion is especially notable in ants such as the clonal raider ant, where local tandem duplication and subsequent dispersed tandem duplication are the primary mechanisms driving gene family expansion [21]. These processes suggest rapid genome evolution and adaptive gene duplication tailored to the needs of social insects, possibly related to their complex social behaviors and communication systems. The origin of the OR gene family in insects is hypothesized to coincide with the evolution of a terrestrial lifestyle in hexapods, indicating that ORs evolved as an adaptation to a terrestrial environment rather than winged flight. This hypothesis is supported by the presence of ORs in all analyzed insect genomes analyzed, pointing to a significant evolutionary innovation in the ancestor of all insects [19]. The evolutionary dynamics of OR gene families are influenced by various factors, including positive selection, gene duplication and loss events, and lineage-specific adaptations. In *Drosophila* species, gene duplication events have played a crucial role in acquiring new olfactory functions, with more than half of the duplicated genes remaining as tandem arrays [22].

Our research indicates that while some OR protein motifs are nearly identical, the evolutionary tree divides into multiple subfamilies, which may be attributed to several factors. Functionally conserved proteins may retain specific motif patterns even if their evolutionary pathways differ. Proteins in different subfamilies may exhibit similar or identical motif patterns [23]. Additionally, motif similarity may sometimes reflect paralogous rather than orthologous homology. Although paralogous proteins may share sequence similarity, their evolutionary origins and functions can be entirely different [24].

In summary, the evolutionary relationships of the OR gene family are characterized by extensive expansions and adaptations across different species, highlighting its critical role in olfaction and survival. The evolution of the OR gene family is shaped by genetic duplication events and

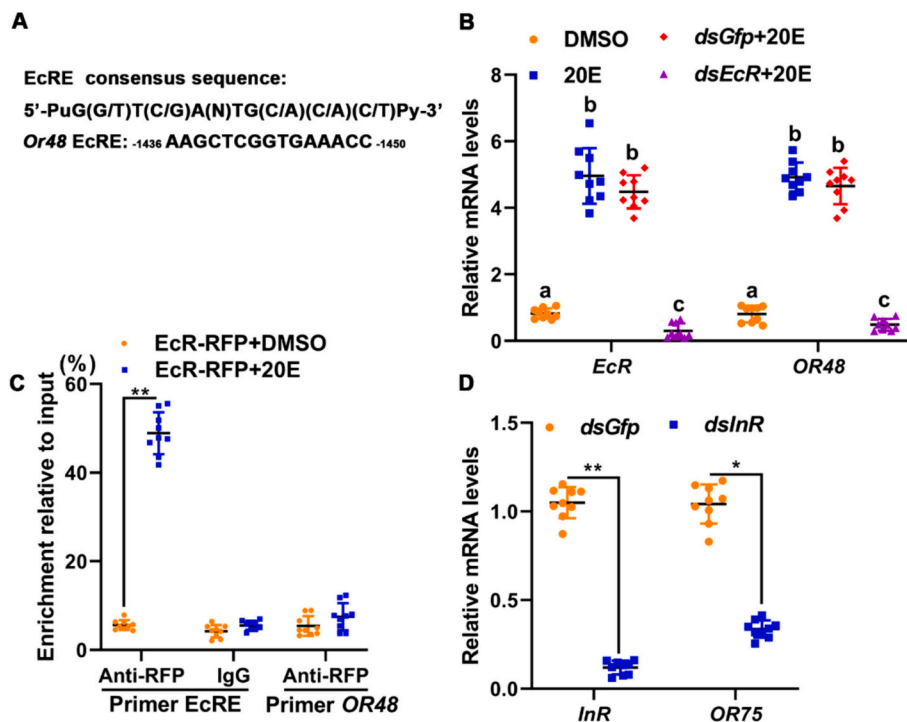


Fig. 7. 20E via EcR promoted *OR48* expression and insulin via InR promoted *OR75* expression. (A) The EcRE site on the *OR48* promoter was predicted using the JASPAR transcription factor database. (B) The expression levels of *EcR* and *OR48* were detected in the antenna after *EcR* knockdown. Statistical analysis was conducted using ANOVA, different letters represented significant differences ($p < 0.05$). The bars indicate the mean \pm standard deviations (SD) of three times repetition. (C) ChIP assay showing 20E promoted *OR48* expression via EcR binding to EcRE and detected by RT-qPCR. IgG is a negative control. Primer *EcRE* targeting EcRE. Primer *OR48*, as non-EcRE control targeting to *OR48* open reading frame (ORF). (D) The expression levels of *InR* and *OR75* were detected in the antenna after *InR* knockdown. Paired data were statistically analyzed using Student's *t*-test; asterisks indicate significant differences ($*p < 0.05$, $**p < 0.01$). The bars in the figures represent the mean standard deviation (SD) for three separate biological experiments.

selective pressures related to ecological specialization and adaptive behaviors [22,25,26].

4.3. Functional diversity of ORs and the expression of ORs under hormone stimulation

In vertebrates, the OR gene family is responsible for the initial step of olfactory discrimination, where specific receptors on the surface of olfactory sensory neurons interact with odorous ligands [17]. This interaction triggers a transduction cascade that ultimately results in the perception of smell. In insects, particularly in *D. melanogaster*, the OR gene family also plays a critical role in olfaction. The identification of thousands of OR genes in *Drosophila* highlights the importance of this gene family in the olfactory systems of these organisms [22]. ORs have long been understood to serve as chemosensors in the olfactory epithelium (OE), where they detect and distinguish volatile odorants. Initially believed to be exclusive to the OE and specific to classic sensory physiology, recent studies have revealed an ectopic expression of ORs in various nonsensory tissues [27–29]. These ectopic ORs are implicated in a range of physiological processes, from adipogenesis to myogenesis to hepatic lipid accumulation to serotonin secretion [30]. They contribute to maintaining oxygen homeostasis, regulating systemic blood pressure, participating in tumor cell proliferation and metastasis, and influencing fetal hemoglobin levels in sickle cell anemia and thalassemia [31]. This highlights the potential therapeutic targets that ectopic ORs represent in non-olfactory tissues.

Insects possess an exceptional olfactory acumen, owing to a diverse array of ORs evolved to decipher crucial olfactory cues vital for their survival [32]. Some *HarmORs* have been identified as larval antennal specific gene in previous works [33]. In this study, *OR48* and *OR75* were also detected in the antenna and other tissues such as the epidermis,

midgut and fat body, albeit at lower expression levels compared to the antenna. These ORs may have roles beyond food finding. The majority of ORs are orphan receptors, lacking known ligands. Moreover, the interaction between ORs and ligands is essential for their function. For instance, the novel receptor clone 29, highly homologous to the rat estrogen receptor (ER), exhibits specific binding affinity for 17 β -estradiol (E2) and stimulates gene transcription in response to E2 [34]. Research has shown that olfactory receptors function by sensing insulin peptide ligands [35], indicating their ability to interact with hormones such as estrogen and insulin. This suggests a mechanism through which hormone stimulation could modulate OR function. We observed that different ORs were regulated by different hormones and played roles in both feeding and non-feeding stages of larvae. *OR75* and *OR48* were identified to be upregulated by insulin and 20E, respectively. These mechanisms are crucial for understanding how ORs respond to hormone stimulation and integrate these signals into cellular responses. Furthermore, we investigated their effects on larval metamorphosis and speculated that they may also influence feeding and metabolism, necessitating further investigation.

5. Conclusions

In summary, we performed a comprehensive characterization of the *HarmOR* gene family and identified 81 *HarmOR* genes in the genome of *H. armigera*. We performed phylogenetic analysis on these genes and further categorized them into 15 groups based on their sequence similarity and evolutionary relationship. We specifically examined *OR48*, which exhibited high expression during metamorphosis stages, and *OR75*, which showed high expression during feeding stages. We observed that 20E increased the expression of *OR48* via ECR and induced the translocation of *OR48* to the cell membrane, while insulin

upregulated the expression of *OR75* via InR. Furthermore, we investigated the functional roles of these genes. *OR48* promotes the pupal process during metamorphosis, promoting autophagy and apoptosis in fat body, while *OR75* slows down the pupation process during feeding stage, significantly inhibiting autophagy and apoptosis in fat body. These findings shed light on the complexity of ORs' function and their potential as therapeutic targets in non-olfactory environments.

Author statement

We confirm that this work is original and has not been published elsewhere, nor is it currently under consideration for publication elsewhere.

CRedit authorship contribution statement

Yanli Li: Investigation, Writing – original draft, Writing – review & editing. **Qichao Chai:** Visualization, Methodology, Validation. **Ying Chen:** Project administration, Supervision. **Yujia Ma:** Formal analysis, Data curation. **Yongcui Wang:** Resources, Software, Project administration. **Junsheng Zhao:** Conceptualization, Supervision, Modified the manuscript, Funding acquisition.

Funding

This work was supported by grants from the Natural Science Foundation of Shandong Province, China (ZR2022QC198), the Agricultural Science and Technology Innovation Project of Shandong Academy of Agricultural Sciences, China (CXGC2023F06), Key Technology Research and Development Program of Shandong (2021LZGC026), “Double-Hundred Talent Plan” Foreign Expert of Shandong Province (WST2020011).

Declaration of competing interest

The authors have no conflict of interest to declare.

Data availability

Data will be made available on request.

Appendix A. Supplementary data

Supplementary data to this article can be found online at <https://doi.org/10.1016/j.ijbiomac.2024.134646>.

References

- N.E. Stork, How many species of insects and other terrestrial arthropods are there on earth? *Annu. Rev. Entomol.* 63 (2018) 31–45.
- X.-f. Zhao, Progress in understanding hormonal regulation during the postembryonic development of *Helicoverpa armigera*, *J Integr Agr* 19(6) (2020) 1417–1428.
- S. Li, X. Yu, Q. Feng, Fat body biology in the last decade, *Annu. Rev. Entomol.* 64 (2019) 315–333.
- C.Y. Liu, W. Liu, W.L. Zhao, J.X. Wang, X.F. Zhao, Upregulation of the expression of prodeath serine/threonine protein kinase for programmed cell death by steroid hormone 20-hydroxyecdysone, *Apoptosis* 18 (2) (2013) 171–187.
- X.P. Wang, Z. Huang, Y.L. Li, K.Y. Jin, D.J. Dong, J.X. Wang, X.F. Zhao, Kruppel-like factor 15 integrated autophagy and gluconeogenesis to maintain glucose homeostasis under 20-hydroxyecdysone regulation, *PLoS Genet.* 18 (6) (2022) e1010229.
- J.P. Cunningham, M.P. Zalucki, Understanding heliothine (Lepidoptera: Heliothinae) pests: what is a host plant? *J. Econ. Entomol.* 107 (3) (2014) 881–896.
- K. Touhara, S. Sengoku, K. Inaki, A. Tsuboi, J. Hirono, T. Sato, H. Sakano, T. Haga, Functional identification and reconstitution of an odorant receptor in single olfactory neurons, *Proc. Natl. Acad. Sci. U. S. A.* 96 (7) (1999) 4040–4045.
- Z. Yang, J. Cheng, P. Shang, J.P. Sun, X. Yu, Emerging roles of olfactory receptors in glucose metabolism, *Trends Cell Biol.* 33 (6) (2023) 463–476.
- M. Guo, Q. Chen, Y. Liu, G. Wang, Z. Han, Chemoreception of mouthparts: sensilla morphology and discovery of chemosensory genes in proboscis and labial palps of adult *Helicoverpa armigera* (Lepidoptera: Noctuidae), *Front. Physiol.* 9 (2018) 970.
- H. Guo, P.P. Guo, Y.L. Sun, L.Q. Huang, C.Z. Wang, Contribution of odorant binding proteins to olfactory detection of (Z)-11-hexadecenal in *Helicoverpa armigera*, *Insect Biochem. Mol. Biol.* 131 (2021) 103554.
- Y. Chen, P.C. Wang, S.S. Zhang, J. Yang, G.C. Li, L.Q. Huang, C.Z. Wang, Functional analysis of a bitter gustatory receptor highly expressed in the larval maxillary galea of *Helicoverpa armigera*, *PLoS Genet.* 18 (10) (2022) e1010455.
- S. Wang, M. Minter, R.A. Homem, L.V. Michaelson, H. Venthur, K.S. Lim, A. Withers, J. Xi, C.M. Jones, J.J. Zhou, Odorant binding proteins promote flight activity in the migratory insect, *Helicoverpa armigera*, *Mol Ecol* 29 (19) (2020) 3795–3808.
- M. Liu, C. Udhe-Stone, C.T. Goudar, Progress curve analysis of qRT-PCR reactions using the logistic growth equation, *Biotechnol. Prog.* 27 (5) (2011) 1407–1414.
- Y.Q. Di, Y.M. Zhao, K.Y. Jin, X.F. Zhao, Subunit P60 of phosphatidylinositol 3-kinase promotes cell proliferation or apoptosis depending on its phosphorylation status, *PLoS Genet.* 17 (4) (2021) e1009514.
- Y.L. Li, Y.X. Yao, Y.M. Zhao, Y.Q. Di, X.F. Zhao, The steroid hormone 20-hydroxyecdysone counteracts insulin signaling via insulin receptor dephosphorylation, *J. Biol. Chem.* 296 (2021) 100318.
- Y.Q. Di, X.L. Han, X.L. Kang, D. Wang, C.H. Chen, J.X. Wang, X.F. Zhao, Autophagy triggers CTSD (cathepsin D) maturation and localization inside cells to promote apoptosis, *Autophagy* 17 (5) (2021) 1170–1192.
- P. Mombaerts, Molecular biology of odorant receptors in vertebrates, *Annu. Rev. Neurosci.* 22 (1999) 487–509.
- D.S. Hekmat-Scafe, C.R. Scafe, A.J. McKinney, M.A. Tanouye, Genome-wide analysis of the odorant-binding protein gene family in *Drosophila melanogaster*, *Genome Res.* 12 (9) (2002) 1357–1369.
- P. Brand, H.M. Robertson, W. Lin, R. Pothula, W.E. Klingeman, J.L. Jurat-Fuentes, B.R. Johnson, The origin of the odorant receptor gene family in insects, *Elife* 7 (2018).
- P. Mombaerts, The human repertoire of odorant receptor genes and pseudogenes, *Annu. Rev. Genomics Hum. Genet.* 2 (2001) 493–510.
- S.K. McKenzie, D.J.C. Kronauer, The genomic architecture and molecular evolution of an odorant receptors, *Genome Res.* 28 (11) (2018) 1757–1765.
- S. Guo, J. Kim, Molecular evolution of *Drosophila* odorant receptor genes, *Mol. Biol. Evol.* 24 (5) (2007) 1198–1207.
- H.X. Ta, P. Koskinen, L. Holm, A novel method for assigning functional linkages to proteins using enhanced phylogenetic trees, *Bioinformatics* 27 (5) (2011) 700–706.
- M.E. Peterson, F. Chen, J.G. Saven, D.S. Roos, P.C. Babbitt, A. Sali, Evolutionary constraints on structural similarity in orthologs and paralogs, *Protein Sci.* 18 (6) (2009) 1306–1315.
- C. Smadja, P. Shi, R.K. Butlin, H.M. Robertson, Large gene family expansions and adaptive evolution for odorant and gustatory receptors in the pea aphid, *Acyrtosiphon pisum*, *Mol Biol Evol* 26 (9) (2009) 2073–2086.
- F.G. Vieira, J. Rozas, Comparative genomics of the odorant-binding and chemosensory protein gene families across the Arthropoda: origin and evolutionary history of the chemosensory system, *Genome Biol. Evol.* 3 (2011) 476–490.
- M. Spehr, G. Gisselmann, A. Poplawski, J.A. Riffell, C.H. Wetzel, R.K. Zimmer, H. Hatt, Identification of a testicular odorant receptor mediating human sperm chemotaxis, *Science* 299 (5615) (2003) 2054–2058.
- J.L. Pluznick, R.J. Protzko, H. Gevorgyan, Z. Peterlin, A. Sipos, J. Han, I. Brunet, L. X. Wan, F. Rey, T. Wang, S.J. Firestein, M. Yanagisawa, J.I. Gordon, A. Eichmann, J. Peti-Peterdi, M.J. Caplan, Olfactory receptor responding to gut microbiota-derived signals plays a role in renin secretion and blood pressure regulation, *Proc. Natl. Acad. Sci. U. S. A.* 110 (11) (2013) 4410–4415.
- C. Wu, Y. Jia, J.H. Lee, Y. Kim, S. Sekharan, V.S. Batista, S.J. Lee, Activation of OR1A1 suppresses PPAR-gamma expression by inducing HES-1 in cultured hepatocytes, *Int. J. Biochem. Cell Biol.* 64 (2015) 75–80.
- T. Tong, Y. Wang, S.G. Kang, K. Huang, Ectopic odorant receptor responding to flavor compounds: versatile roles in health and disease, *Pharmaceutics* 13 (8) (2021).
- Z. Chen, H. Zhao, N. Fu, L. Chen, The diversified function and potential therapy of ectopic olfactory receptors in non-olfactory tissues, *J. Cell. Physiol.* 233 (3) (2018) 2104–2115.
- J.A. Cheema, C. Carraher, N.O.V. Plank, J. Travas-Sejdic, A. Kralicek, Insect odorant receptor-based biosensors: current status and prospects, *Biotechnol. Adv.* 53 (2021) 107840.
- N.Y. Liu, W. Xu, A. Papanicolaou, S.L. Dong, A. Anderson, Identification and characterization of three chemosensory receptor families in the cotton bollworm *Helicoverpa armigera*, *BMC Genomics* 15 (1) (2014) 597.
- G.G. Kuiper, E. Enmark, M. Pelto-Huikko, S. Nilsson, J.A. Gustafsson, Cloning of a novel receptor expressed in rat prostate and ovary, *Proc. Natl. Acad. Sci. U. S. A.* 93 (12) (1996) 5925–5930.
- J. Cheng, Z. Yang, X.Y. Ge, M.X. Gao, R. Meng, X. Xu, Y.Q. Zhang, R.Z. Li, J.Y. Lin, Z.M. Tian, J. Wang, S.L. Ning, Y.F. Xu, F. Yang, J.K. Gu, J.P. Sun, X. Yu, Autonomous sensing of the insulin peptide by an olfactory G protein-coupled receptor modulates glucose metabolism, *Cell Metab.* 34 (2) (2022) 240–255 e10.
- P. Artimo, M. Jonnalagedda, K. Arnold, D. Baratin, G. Csardi, E. de Castro, S. Duvaud, V. Flegel, A. Fortier, E. Gasteiger, A. Grosdidier, C. Hernandez, V. Ioannidis, D. Kuznetsov, R. Liechi, S. Moretti, K. Mostaguir, N. Redaschi, G. Rossier, I. Xenarios, H. Stockinger, ExPASy: SIB bioinformatics resource portal, *Nucleic Acids Res.* 40 (2012) W597–603 (Web Server issue).

- [37] P. Horton, K.J. Park, T. Obayashi, N. Fujita, H. Harada, C.J. Adams-Collier, K. Nakai, WoLF PSORT: protein localization predictor, *Nucleic Acids Res.* 35 (2007) W585–7 (Web Server issue).
- [38] K. Tamura, G. Stecher, S. Kumar, MEGA11: Molecular evolutionary genetics analysis version 11, *Mol. Biol. Evol.* 38 (7) (2021) 3022–3027.
- [39] I. Letunic, P. Bork, Interactive Tree Of Life (iTOL) v5: an online tool for phylogenetic tree display and annotation, *Nucleic Acids Res.* 49 (W1) (2021) W293–W296.
- [40] R.E. Voorrips, MapChart: software for the graphical presentation of linkage maps and QTLs, *J. Hered.* 93 (1) (2002) 77–78.
- [41] Y. Wang, H. Tang, J.D. DeBarry, X. Tan, J. Li, X. Wang, T.H. Lee, H. Jin, B. Marler, H. Guo, J.C. Kissinger, A.H. Paterson, MCScanX: a toolkit for detection and evolutionary analysis of gene synteny and collinearity, *Nucleic Acids Res.* 40 (7) (2012) e49.
- [42] M. Krzywinski, J. Schein, I. Birol, J. Connors, R. Gascoyne, D. Horsman, S.J. Jones, M.A. Marra, Circos: an information aesthetic for comparative genomics, *Genome Res.* 19 (9) (2009) 1639–1645.
- [43] D. Szklarczyk, J.H. Morris, H. Cook, M. Kuhn, S. Wyder, M. Simonovic, A. Santos, N.T. Doncheva, A. Roth, P. Bork, L.J. Jensen, C. von Mering, The STRING database in 2017: quality-controlled protein-protein association networks, made broadly accessible, *Nucleic Acids Res.* 45 (D1) (2017) D362–D368.
- [44] H.L. Shao, W.W. Zheng, P.C. Liu, Q. Wang, J.X. Wang, X.F. Zhao, Establishment of a new cell line from lepidopteran epidermis and hormonal regulation on the genes, *PLoS One* 3 (9) (2008) e3127.
- [45] W.A. Malik, X. Wang, X. Wang, N. Shu, R. Cui, X. Chen, D. Wang, X. Lu, Z. Yin, J. Wang, W. Ye, Genome-wide expression analysis suggests glutaredoxin genes response to various stresses in cotton, *Int. J. Biol. Macromol.* 153 (2020) 470–491.
- [46] S. Zhu, X. Wang, W. Chen, J. Yao, Y. Li, S. Fang, Y. Lv, X. Li, J. Pan, C. Liu, Q. Li, Y. Zhang, Cotton DMP gene family: characterization, evolution, and expression profiles during development and stress, *Int. J. Biol. Macromol.* 183 (2021) 1257–1269.
- [47] S. Zozulya, F. Echeverri, T. Nguyen, The human olfactory receptor repertoire, *Genome Biol.* 2 (6) (2001). RESEARCH0018.
- [48] X. Zhang, S. Firestein, The olfactory receptor gene superfamily of the mouse, *Nat. Neurosci.* 5 (2) (2002) 124–133.
- [49] L. Buck, R. Axel, A novel multigene family may encode odorant receptors: a molecular basis for odor recognition, *Cell* 65 (1) (1991) 175–187.
- [50] Y. Zhang, B. Wang, Y. Zhou, M. Liao, C. Sheng, H. Cao, Q. Gao, Identification and characterization of odorant receptors in *Plutella xylostella* antenna response to 2,3-dimethyl-6-(1-hydroxy)-pyrazine, *Pestic. Biochem. Physiol.* 194 (2023) 105523.
- [51] O. Mendivil Ramos, D.E. Ferrier, Mechanisms of gene duplication and translocation and progress towards understanding their relative contributions to animal genome evolution, *Int. J. Evol. Biol.* 2012 (2012) 846421.
- [52] S.L. Sullivan, M.C. Adamson, K.J. Ressler, C.A. Kozak, L.B. Buck, The chromosomal distribution of mouse odorant receptor genes, *Proc. Natl. Acad. Sci. U S A* 93 (2) (1996) 884–888.
- [53] M.H. Nagai, L.M. Armelin-Correa, B. Malnic, Monogenic and monoallelic expression of odorant receptors, *Mol. Pharmacol.* 90 (5) (2016) 633–639.
- [54] A. Couto, M. Alenius, B.J. Dickson, Molecular, anatomical, and functional organization of the *Drosophila* olfactory system, *Curr. Biol.* 15 (17) (2005) 1535–1547.
- [55] J.S. Lobmaier, U. Fischbacher, U. Wirthmuller, D. Knoch, The scent of attractiveness: levels of reproductive hormones explain individual differences in women's body odour, *Proc. Biol. Sci.* 285 (1886) (2018).
- [60] A.L. Cerda-Molina, L. Hernandez-Lopez, O.C. de la, R. Chavira-Ramirez, R. Mondragon-Ceballos, Changes in men's salivary testosterone and cortisol levels, and in sexual desire after smelling female axillary and vulvar scents, *Front. Endocrinol. (Lausanne)* 4 (2013) 159.